

Bioactive Interpenetrating Polymeric Networks: Incorporation of *Hibiscus sabdariffa* Polyphenols for Enhanced Biocompatibility and Mechanical Properties

Martín Caldera-Villalobos*, Jesús A. Claudio-Rizo

Facultad de Ciencias Químicas. Universidad Autónoma de Coahuila. Unidad Saltillo. Saltillo, Coahuila, 25280, México.

*Corresponding author: Martín Caldera-Villalobos, email: caldera_martin@hotmail.com

Received July 2nd, 2024; Accepted October 3rd, 2024.

DOI: <http://dx.doi.org/10.29356/jmcs.v69i3.2331>

Abstract. The synthesis and characterization of bioactive interpenetrating polymeric networks (IPNs) made from collagen, polyurethane, and polyphenols extracted from *Hibiscus sabdariffa* flowers are presented. Polyphenols were extracted via ultrasound-assisted methods and incorporated into IPNs to enhance their properties. The study explored various IPN compositions and assessed their physicochemical characteristics, including thermal stability, mechanical properties, swelling behavior, and degradation in different media. FTIR analysis confirmed the presence of phenolic and collagen components in the polymer networks. Thermogravimetric analysis indicated a decrease in thermal stability with higher polyphenol content, attributed to lower crosslinking density. Rheometry showed an increase in storage modulus with polyphenol incorporation, suggesting enhanced mechanical strength. Swelling studies demonstrated that polyphenol-enriched IPNs exhibit higher water absorption, especially in alkaline conditions. Biocompatibility tests, including MTT and hemolysis assays, revealed favorable interactions with human monocytes and porcine fibroblasts. The findings suggest that *Hibiscus sabdariffa* polyphenols can significantly improve the bioactivity and mechanical properties of IPNs, making them suitable for biomedical applications, particularly in wound healing and tissue engineering.

Keywords: Biocompatible polymers; biobased polymers; biodegradable polymers; collagen; polyurethane.

Resumen. Este trabajo presenta la síntesis y caracterización de redes poliméricas interpenetradas (IPN) bioactivas elaboradas a partir de colágeno, poliuretano y polifenoles extraídos de flores de *Hibiscus sabdariffa*. Los polifenoles se extrajeron en un proceso asistido por ultrasonido y se incorporaron a las IPNs para mejorar sus propiedades. El estudio exploró varias composiciones de IPNs y evaluó sus características fisicoquímicas, incluida la estabilidad térmica, las propiedades mecánicas, el comportamiento de hinchamiento y la degradación en diferentes medios. El análisis por FTIR confirmó la presencia de componentes fenólicos y de colágeno en las redes de polímeros. El análisis termogravimétrico indicó una disminución en la estabilidad térmica con un mayor contenido de polifenoles, atribuido a una menor densidad de reticulación. La reometría mostró un aumento en el módulo de almacenamiento con la incorporación de polifenoles, lo que sugiere una mayor resistencia mecánica. Los estudios de hinchamiento demostraron que las IPN enriquecidas con polifenoles exhiben una mayor absorción de agua, especialmente en condiciones alcalinas. Las pruebas de biocompatibilidad, incluidos MTT y ensayos de hemólisis, revelaron interacciones favorables con monocitos y eritrocitos humanos y fibroblastos porcinos. Los hallazgos sugieren que los polifenoles de *Hibiscus sabdariffa* pueden mejorar significativamente la bioactividad y las propiedades mecánicas de las IPN, haciéndolas adecuadas para aplicaciones biomédicas, particularmente en la curación de heridas y la ingeniería de tejidos.

Palabras clave: Polímeros biocompatibles; polímeros bio-basados; polímeros biodegradables; colágeno; poliuretano.

Introduction

Phenolic resin molding compounds have been widely used due to their strength, heat resistance, long-term reliability, and cost-effectiveness.[1] However, the use of petroleum-based thermosets is limited by fossil fuel depletion and environmental concerns.[2] Traditional phenolic thermosets are synthesized from toxic precursors like phenol and formaldehyde.[3] To address this, bio-based and non-toxic alternatives are being developed. Bio-based phenol-formaldehyde resins from sustainable biomass are promising substitutes as they are less contaminating.[4]

Phenolic resins are valued for their thermal stability, chemical resistance, fire resistance, and dimensional stability. Researchers have replaced phenol with sustainable materials such as lignin, tannin, or cardanol. [5] Phenolic resins have also been synthesized from bio-oil compounds like *o*-cresol, *m*-cresol, and *p*-cresol. [6] Resveratrol-based resins offer low thermal expansion and superior heat resistance compared to commercial phenolic resins. [7]

Incorporating lignin micro and nanoparticles as fillers in phenol-formaldehyde adhesives improves thermal resistance and adhesion. [8] Lignin, a natural phenolic polymer, can be sourced from materials like palm kernel shell and rice husk. 2 Vanillin and guaiacol from lignin are used to create eco-friendly flame retardants for epoxy resins. [9] These resins also exhibit low dielectric properties and have been used as fireproof coatings for wood. [10] Tannins from *Acacia mearnsii* bark have been copolymerized with phenol-formaldehyde for plywood adhesives, enhancing resin properties. [11,12]

Natural phenolic compounds are key to a sustainable plastic industry and new biomaterials. [13] Bio-based materials are often biocompatible and biodegradable, with polyphenols showing broad biological activity. [14] Polyphenols, including flavonoids and phenolic acids, are used in wound healing. [15] Hydroxycinnamic acids and derivatives are potential alternative drugs for skin disorders, promoting fibroblast and keratinocyte proliferation. [16] Anthocyanins have antioxidant and anti-inflammatory properties beneficial for wound healing.[17]

Hibiscus sabdariffa, rich in phytochemicals like anthocyanins and organic acids, is used in traditional medicine and has potential modern therapeutic applications.[18] Studies show its antioxidant, anti-inflammatory, cytotoxic, and antimicrobial activities.[19] Hibiscus leaf compounds inhibit endothelial cell oxidative injury and LDL oxidation.[20]

Fig. 1 illustrates the chemical structures of *Hibiscus sabdariffa* flower constituents, including delphinidin-3-sambubioside, cyanidin-3-sambubioside, 3,4-dihydroxybenzoic acid, hibiscetin, and gossypetin.21 These compounds can be used as monomers for bio-based and bioactive phenolic polymers.

Interpenetrating polymer networks (IPNs) represent a category of polymer materials consisting of two or more polymeric systems that are cross-linked and interwoven at the molecular scale.[22] They are synthesized by the sequential polymerization of monomers able to form polymer networks, yielding materials which can be considered as polymer alloys. IPNs shows excellent thermal and mechanical properties.[23,24] Researchers have employed network design strategies to overcome the weak mechanical properties of traditional hydrogels, which often result in failure, with an emphasis on enhancing extensibility and fracture resistance.[25]

Phenolic resins for biological applications require controlled degradation. Our research group reported biocompatibility of polymer networks made of collagen, alginate, and polyurethane. [26] Alginate-polyurethane networks in water are useful for biomedical hydrogels. [27] Combining hydrogels with polyphenols can enhance wound healing, tissue regeneration, and anti-inflammatory effects. [28] This study aims to evaluate the effect of polyphenols from *Hibiscus sabdariffa* flowers on the properties of bio-based polymer networks of collagen, polyurethane, and phenolic polymers.

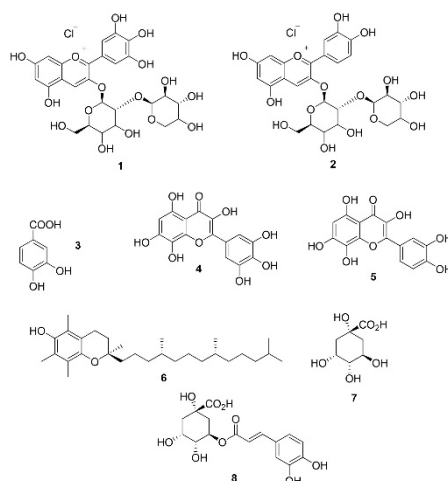


Fig. 1. Chemical structures of major constituents in *Hibiscus sabdariffa* flower extract.

Experimental

Chemicals

Phenol (99 %), formaldehyde (37 % aqueous solution), sodium hydroxide (98 %), glycerol ethoxylate ($M_n \approx 1000 \text{ g mol}^{-1}$), hexamethylene diisocyanate (99 %), sodium metabisulfite (99 %), Folin-Ciocalteu's phenol reagent, sodium carbonate (99 %), aluminum chloride (99 %), ethanol (HPLC grade > 99.999 %), methanol (HPLC grade > 99.999 %), acetic acid (99.7 %), and rhodamine B (95 %) were purchased from Sigma Aldrich and used without further purification. Collagen was extracted from porcine dermis by enzymatic hydrolysis as reported. Polyurethane with blocked isocyanate groups was synthesized from glycerol ethoxylate and hexamethylene diisocyanate as reported.

Extraction of polyphenols

Polyphenols were extracted by an ultrasound assisted process. 20 g of dried flowers (purchased from a local market) were washed with distilled water and placed in a beaker with 200 mL of EtOH:H₂O (7:3). The mixture was sonicated at 60 °C for 2 h and then flowers were removed, and the resulting solution was filtered under vacuum. The volume of solution was adjusted to 250 mL yielding a concentration of 3.2 wt.%. Total polyphenols in the extract were measured by the Folin-Ciocalteu's method. For this, a solution of 10 mg mL⁻¹ of the extract was prepared in distilled water. Also, 2 wt.% Na₂CO₃ and 10 wt.% Folin-Ciocalteu's reagent solutions were prepared in deionized water. Samples were prepared by mixing 40 μL of extract solution, 80 μL of Na₂CO₃ solution, and 100 μL of Folin-Ciocalteu's reagent solution. The reaction proceeded by 15 min at room temperature and then the absorbance of samples was measured at 765 nm. Total polyphenols content was calculated comparing results with a calibration curve of gallic acid (0-1000 μg mL⁻¹). Results were expressed as mg gallic acid equivalent per g of dried weight (mg GAE/g dw).

The content of flavonoids was measured by a colorimetric method using aluminum chloride. A suitable reagent for flavonoids was prepared mixing 133 mg of aluminum chloride and 400 mg of sodium acetate in 100 mL of MeOH-H₂O-AcOH (14:5:1). Samples were prepared by mixing 0.1 mL of extract solution, 0.5 mL of reagent for flavonoids, and 1.4 mL of distilled water and they reacted by 30 min at room temperature. Then, the absorbance of samples was measured at 430 nm and the content of flavonoids was calculated comparing results with a calibration curve of quercetin (0-1000 μg mL⁻¹). Results were expressed as mg quercetin equivalent per gram of dried weight (mg QE/g dw). [29,30]

Synthesis of polymer networks

The synthesis of polymer networks (IPN-1, IPN-2, and IPN-3) was performed in a two-step process (Fig. 2). IPN-1 was formulated with phenol, formaldehyde, polyurethane, and collagen. For IPN-2 and IPN-3, phenol was partially substituted with phenols extracted from *Hibiscus sabdariffa*. First, a phenolic polymer was synthesized following the typical procedure to obtain resols. A suitable amount of phenol and/or *Hibiscus sabdariffa* extract was mixed in 25 mL of deionized water and then 100 mg of NaOH was added as the catalyzer. The mixture was heated at 70 °C with continuous stirring and then, 1.48 g of formaldehyde was added, the mixture was reacted by 30 min. Simultaneously, 0.6 g of collagen (aqueous solution 6 mg mL⁻¹) were heated at 70 °C with magnetic stirring in a beaker. Once the phenolic polymer was formed, it was transferred to the beaker containing collagen and the resulting mixture was stirred until obtain a homogeneous mixture. Then, a suitable amount of polyurethane was added with vigorous stirring, and the mixture was reacted by 30 min at 60 °C to obtain the polymer networks. At the end of the reaction the product was filtered and rinsed with deionized water and dried at room temperature. Designations and amounts used for the synthesis of polymer networks are shown in Table 1. Each material was prepared independently in triplicate.

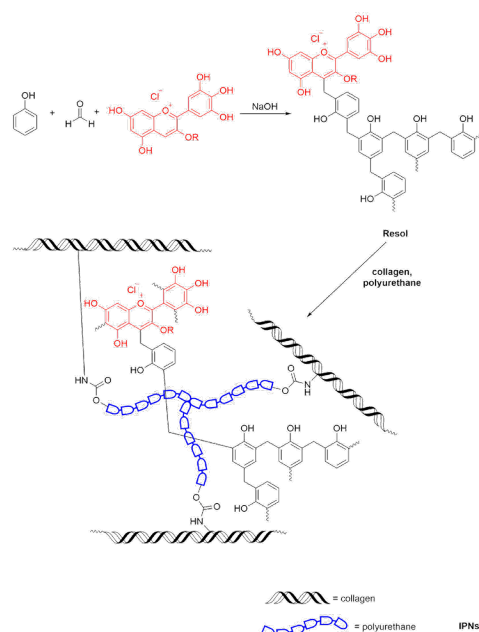


Fig. 2. Synthesis of interpenetrating polymer networks from polyphenols.

Table 1. Quantities of reagents utilized in the synthesis of polymeric networks.

Key	Phenol (g)	<i>Hibiscus sabdariffa</i> extract (g)	Formaldehyde (g)	Collagen (mg)	Polyurethane (mg)	NaOH (mg)
IPN-1	4	0	1.48	600	90	100
IPN-2	3.75	0.25	1.48	600	90	100
IPN-3	3.5	0.5	1.48	600	90	100

Physicochemical characterization

FTIR spectra were recorded with a *Perkin Elmer Frontier* spectrophotometer using an attenuated total reflection (ATR) accessory. Samples were previously dried at room temperature with a desiccator. The storage module (G') and the loss module (G'') of hydrogels were measured by low amplitude oscillatory rheometry using an *Anton-Paar Physica MCR 301* rheometer. Experiments were conducted at 37 °C with a plate-plate geometry (diameter = 40 mm). Measurements were performed with a 10 % of strain to ensure the viscoelastic behavior in the dynamic response of hydrogels.

The degradation behavior of hydrogels was studied in hydrolytic and proteolytic media. The hydrolytic media were aqueous solutions with pH 2, 7.4, and 12. The proteolytic media were aqueous solutions of papain (14 U/gel) and collagenase (14 U/gel). The experiments were performed in closed jars placing a sample of IPN (0.25 g) and 10 mL of the hydrolytic or proteolytic solution. Samples remained in repose at room temperature (25 ± 1 °C) and the mass of hydrogels was monitored at different time intervals. Experiments were performed in triplicate.

Release of polyphenols

To evaluate the release of polyphenols from IPN-2 and IPN-3 samples of these materials (0.25 g) were placed in closed jars with 10 mL of HCl aqueous solutions (pH = 1, 2, 4, and 6, these values were selected to carry out the UV-Vis measurements at the same λ_{\max} , the color of the extract change from red to green at higher values of pH) and they remained a 25 ± 1 °C without stirring. Aliquots (200 μ L) were taken from the medium and their absorbance was measured at 516 nm.

Evaluation of *in vitro* biocompatibility

MTT assay

The variation of metabolism of human monocytes and porcine dermal fibroblasts (got from primary culture) growing on every IPN was assessed. Cell suspensions in DMEM (for fibroblasts) or RPMI (for monocytes) culture medium were added to the wells containing hydrogels (50,000 cells/well) and control (without hydrogels), and these were incubated for 24 and 48 h, respectively. The cell viability was dictated by the limit of cells with dynamic metabolism to transform MTT salts in formazan. The MTT solution (2 wt./v %) was added to wells with polymer networks and controls (PBS-1X), and afterward, the cells were kept up under culture conditions for 2 h at 37 °C. At that point, the medium was tapped, the formazan was diluted in propan-2-ol, and the absorbance of the solutions was measured at 560 nm, using a *ThermoScientific MultiSkanSky* spectrophotometer. Cell viability was calculated with Equation 1:

$$\text{Cell viability \%} = \frac{A_{\text{composite}}}{A_{\text{control}}} * 100 \quad (1)$$

where $A_{\text{composite}}$ and A_{control} are the absorbances for composite hydrogels and control (PBS-1X) respectively.

Hemolysis assay

The hemocompatibility of hydrogels was evaluated by the hemolysis assay measuring the released hemoglobin after destroying the cell membrane of erythrocytes. Samples of erythrocytes previously purified in Alsever's solution (112 μ L) were mixed with 150 μ L of leached extracted from polymer networks, and 1728 μ L of Alsever's solution. Alsever's solution, and deionized water were used as the negative (0 % of hemolysis), and positive (100 % of hemolysis) controls, respectively. Samples were incubated at 37 °C with orbital stirring (250 rpm) for 30 min. After that, samples were centrifugated at 3000 rpm and aliquots were taken from the supernatant. The absorbance of samples was measured at 415 nm with a *ThermoScientific MultiskanSky* spectrophotometer, and the percentage of hemolysis was calculated with Equation 2:

$$\text{Hemolysis (\%)} = \frac{A_{\text{sample}} - A_{\text{control}(-)}}{A_{\text{control}(+)} - A_{\text{control}(-)}} * 100 \quad (2)$$

where A_{sample} , $A_{\text{control}(-)}$ y $A_{\text{control}(+)}$ are the absorbances of samples, negative control, and positive control, respectively.

Cell proliferation

The growing of porcine fibroblasts in contact with the composite hydrogels for 48 h was evaluated with the *Live/Dead* fluorescence assay. Similarly, fibroblasts under the same conditions were stained with rhodamine B. Cell populations and proliferation were observed using a *VELAB VE-146YT* epifluorescence microscope.

Enzyme linked immunosorbent assay

The effect of the composition of the composite hydrogels on cell signaling was evaluated using ELISA for the detection of important cytokines in tissue inflammation and reconstruction processes, such as alpha tumor necrosis factor (TNF- α) and interleukin 10 (IL-10). The cytokines were determined in human monocytes growing in the presence of the composite materials for 48 h following the supplier's instructions (*Invitrogen*). Cells growing in PBS-1X were used as a reference control.

Analysis of data

All experiments were performed independently in triplicate. Average values and standard deviations are presented. Variability between data is analyzed with one-way ANOVA. Statistically significant differences were determined using the Tukey test ($p < 0.05$). In the line dot graphs, the standard deviation bar is not presented in the graphs to avoid losing trends between the groups being compared.

Results and discussion

Characterization of polymer networks

The chemical structure of polymer networks was analyzed by FTIR (Fig. 3(b)). The spectra of IPN-1, IPN-2, and IPN-3 showed some typical bands for phenol, collagen, and polyurethane. However, the spectra of IPN-2 and IPN-3 showed some weakened bands related to phenol due to the partial substitution of this compound by polyphenols extracted from *Hibiscus sabdariffa*. The absorption band in 3280 cm^{-1} was assigned to the $\nu\text{ArO-H}$ vibration due to the phenolic polymers incorporated in the polymer networks. Another band related with phenolic compounds was observed in 1500 cm^{-1} which is due to the $\nu\text{C-C}$ vibration. For IPN-2 and IPN-3 an absorption band in 1230 cm^{-1} was observed and it was attributed to the Ar-O-R stretching from glycosylated polyphenols occurring in the *Hibiscus sabdariffa* extract. The presence of collagen in the polymer networks was confirmed by the presence of the amide I and amide II bands in 1640 and 1540 cm^{-1} which are related with the polypeptide backbone. Further, a band in 1030 cm^{-1} was assigned to the C-O and C-N stretching vibrations from amino and carboxylic acid residues occurring in collagen. The formation of the polymer networks was confirmed by the band in 1730 cm^{-1} which is due to the $\nu\text{C=O}$ vibration from urea and urethane groups which results from the reaction of isocyanate with amino or hydroxyl groups, respectively. Also, a band in 1099 cm^{-1} due to the R-O-R stretching from the polyurethane backbone was observed.

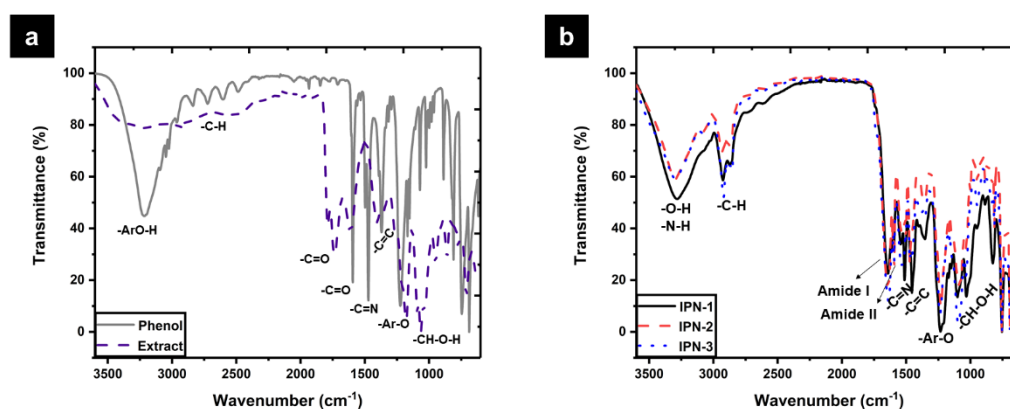


Fig. 3. FTIR spectra of: (a) *Hibiscus sabdariffa* extract vs. phenol, and (b) synthesized polymer networks.

Polymer networks are characterized by a high crosslinking degree and thus, by a high thermal, mechanical, and chemical stability. Thermal stability of polymer networks was analyzed by TGA and the thermograms are shown in Fig. 4(a). The dehydration temperature (10 % weight loss) for IPN-1, IPN-2, and IPN-3, was 236, 185, and 206 °C, respectively. Thermal degradation of polymer networks take place in two stages. The first weight loss in the range of 50 to 250 °C was attributed to the evaporation of physically adsorbed water, and the second in the range of 250 to 600 °C corresponded to the exothermal decomposition by the random scission of polymer chains. Results showed that the incorporation of polyphenols in the polymer networks do not contribute to improve the thermal stability. Conversely, the degradation temperature of IPN-1 decreases from 422 °C to 363 and 386 °C for IPN-2 and IPN-3, respectively. Also, the residual weight corresponding to ashes obtained after calcination at 800 °C was 33.4, 19.8 and 15.8 % for IPN-1, IPN-2, and IPN-3, respectively. This shows that increasing the concentration of polyphenols in the polymer networks the thermal stability decreases.

Phenol-formaldehyde resins typically have a high crosslinking degree due the high reactivity of phenol towards the electrophilic substitution in the positions 2, 4 and 6 acting as a trifunctional monomer. The loss of thermal stability could be attributed to the high tendency towards oxidation of polyphenols. However, a lower crosslinking degree could contribute to decrease the thermal stability of polymer networks. A theoretical analysis made by the density functional theory (DFT) of the reactivity of delphinidin-3-sambubioside showed that their main reactive sites are localized in C4, C8, O4', and O7 (Fig. 4(b)). Only C4 is activated as an electrophilic site while C8 is activated as a nucleophilic site [31]. Thus, incorporating polyphenols such as delphinidin and cyanidin in the phenolic prepolymers decreases the degree of polymerization because they contribute with only one electrophilic site while phenol provides three electrophilic sites. Thus, these polyphenols decrease the crosslinking degree of the resulting polymer networks decreasing their thermal stability as well. O4' and O7 are activated for the nucleophilic attack, and they are suitable to conduct reactions like esterification. The high rigidity of the polyphenolic component prevents crosslinking with the collagen fibers interpenetrated with polyurethane. Indicating that a large part of the extract used remains physically loaded in the IPN collagen-polyurethane matrix, which is evident since IPN-3 showed greater mass loss in the first region.

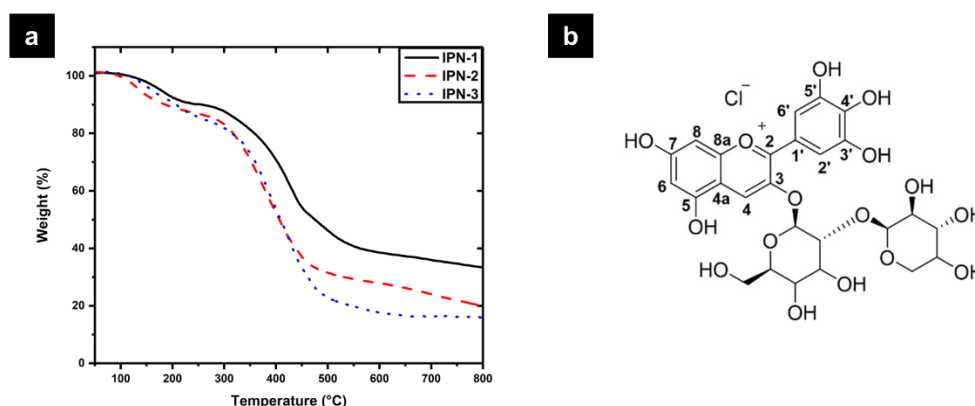


Fig. 4. (a) TGA thermograms of polymer networks and **(b)** labeled structure of delphinidin-3-sambubioside.

Mechanical stability of polymer networks was evaluated by oscillatory rheometry measuring the storage modulus and the loss modulus (Fig. 5). For the three polymer networks, the storage modulus is higher than the loss modulus showing the typical behavior of hydrogels where the elastic behavior dominates over the viscous behavior. At a frequency of 10 Hz the storage modulus of IPN was 837 Pa for IPN-1, while G' for IPN-2 was 7930 Pa, and 1640 Pa for IPN-3, which represents an increase of 847 and 95 % respect to IPN-1. The incorporation of polyphenols in polymer networks could increase the rigidity of polymer chains due to the presence of large and voluminous moieties, contributing to reinforce the resistance to the deformation of the matrix. Also, the intermolecular forces such as hydrogen bonding and π - π interactions established by polyphenolic moieties of the network could enhance the mechanical strength of polymer networks. However,

if a high amount of polyphenols is used (in the IPN-3 case), some are not incorporated into the network but are trapped in the network, causing a decrease in the storage modulus.

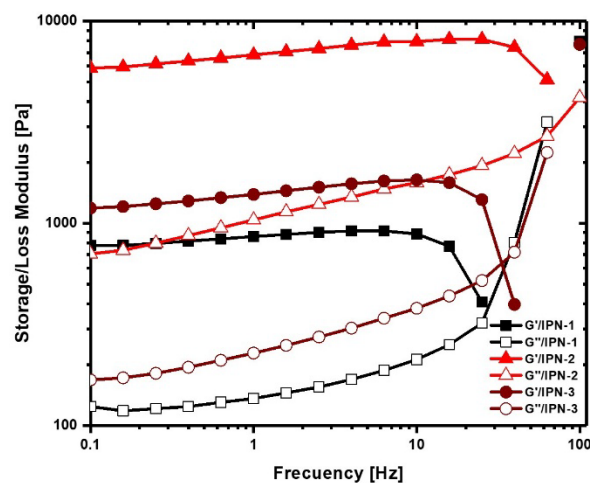


Fig. 5. Viscoelastic behavior of polymer networks analyzed by oscillatory rheometry.

Swelling and degradation behavior

Fig. 6 shows the swelling/degradation profiles of polymer networks in hydrolytic and proteolytic media. IPN-1 in acid medium showed a low swelling capacity, the polymer matrix was progressively swelling during the first seven days of contact reaching a 122 ± 1 % of swelling, then remained without significant variation without degradation. IPN-2 swelled more rapidly than IPN-1, the maximum swelling was observed after 10 days of contact (447 ± 1 % of swelling) followed by the accelerated loss weight until being completely degraded at the fourteenth day. IPN-3 reached a 204 % of swelling during the first 24 h of contact with HCl solution, followed by a drastic weight loss in the next 24 h. Then, the mass of the hydrogels remained almost constant for 11 days and finally after 14 days of contact were completely degraded. The residues obtained after 30 days in contact with hydrolytic and proteolytic media were analyzed by FTIR (spectra are provided in the supporting information) to understand the nature of the degradation process. The most significant changes in the FTIR spectra of IPN-2 and IPN-3 were the absence of the absorption bands at 1590 and 1500 cm^{-1} due to the release of aromatic compounds such as polyphenols.

The three polymer networks showed a similar behavior in alkaline medium, swelling during the first 6-7 days and remaining without significant mass variation during the posterior days. The swelling capacity decrease in the order IPN-3 > IPN-2 > IPN-1 showing that polyphenols from *Hibiscus sabdariffa* enhances the water absorption capacity of polymer networks. In general, polymer networks showed higher swelling degree in alkaline medium compared with acid medium. This could be attributed to the weak acid character of phenolic compounds. The pK_a of phenol is 9.99 and thus at pH 12 phenolic moieties are deprotonated acquiring negative charge. The electrostatic repulsion between negatively charged chains favors the water absorption inside the polymer matrix and increasing the swelling degree. At the end of the experiment, the FTIR spectra did not show significant changes, indicating that the polyphenols remain inside the IPN in alkaline medium.

Similarly, IPN-2 and IPN-3 showed better swelling behavior and hydrolytic stability than IPN-1 in PBS-1X (pH = 7.4). The maximum swelling capacity for IPN-1 was 85 ± 1 % after 24 h of contact with the saline solution. After, that the hydrogels began to lose weight due to the progressive hydrolytic degradation being completely degraded after 22 days. For IPN-1, a decrease in the absorption band of amide I was observed disappearing almost for complete. This result indicate that collagen is the component most susceptible to being hydrolyzed in PBS-1X. There was not observed significant changes in the other bands of the spectrum, showing that the phenolic polymer and the polyurethane are not affected by the hydrolytic degradation.

The maximum swelling degree of IPN-3 in papain was 367 ± 2 % after 10 days of contact. Then, a progressive weight loss was observed but the material was not completely degraded after 30 days of contact with papain. In collagenase, a noticeable degradation was not observed for IPN-3. In proteolytic media, IPN-1 showed a low water absorption capacity reaching a 151 ± 1 % in papain and 125 ± 1 % in collagenase during the first 24 h. Then, samples were progressively degraded by the action of both enzymes which cleavage the peptide bond of collagen. This was confirmed by the absence of the amide I band in the FTIR spectrum which is typical of the collagen backbone. Finally, for IPN-2, the effects of proteolytic degradation were not noticeable. The presence of polyphenols in IPN improves resistance to proteolytic degradation. This could be used for wound healing dressings with resistance to degradation for extended periods of use.

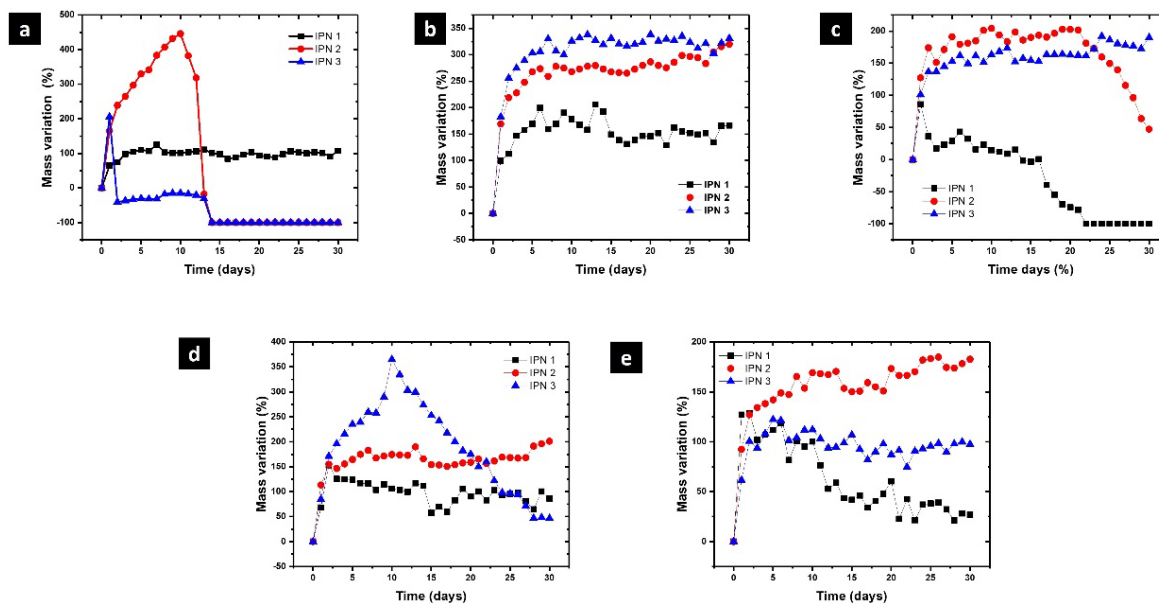


Fig. 6. Swelling/degradation profiles of polymer networks in: (a) 0.1 M HCl, (b) 0.1 M NaOH, (c) PBS-1X, (d) papain, and (e) collagenase.

Polyphenols release

Due to their high biological activity, polyphenols are an efficient alternative to synthetic compounds, responding to the need to find new options for chronic wound care. Nonetheless, polyphenols have some drawbacks when targeting wound applications, such as low stability and consequent decreased biological performance at the wound site. These limitations have been overcome using polymeric-based systems as carriers of polyphenols for wound healing, improving its stability, controlling the release kinetics, and therefore increasing the performance and effectiveness [32]. As polymer networks are progressively degraded, some polyphenols are released to the medium. This process was monitored by UV-Vis spectroscopy and the concentration profiles at different values of pH are shown in Fig. 7. IPN-2 shows the maximum release of polyphenols reaching a concentration of 0.5 mg cm^{-3} after 12 days at pH 6. These results are relevant because the pH of skin and blood is acid, being a favorable environment for the release of polyphenols during wound healing. The high structural rigidity is associated with the decrease in the release of polyphenols reaching 0.2 mg cm^{-3} after 12 days at pH 4. The release of polyphenols is important to describe the biocompatibility of these polymer networks because they are biologically active compounds.

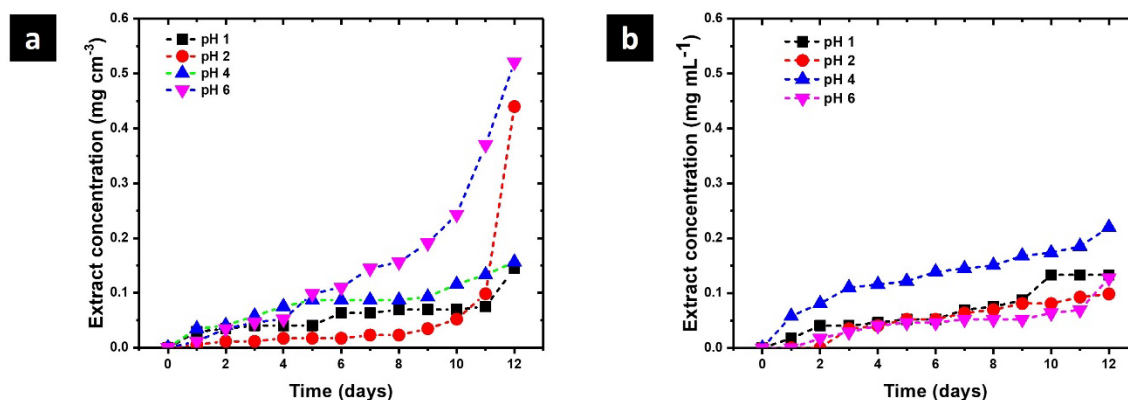


Fig. 7. Polyphenols release profiles for (a) IPN-2 and (b) IPN-3.

Evaluation *in vitro* of biocompatibility

Cell viability

The cytotoxic character of polymer networks was evaluated by the MTT assay. Fig. 8 shows that the increase in viability in porcine samples was from 20 to 80 % compared to the control sample. In the case of human monocytes, it was more than 40 % in some cases and in others less than 20 % compared to the control. According with Chowdhury et al., polyphenols increase the deposition of collagen and elastin by human dermal fibroblasts during the wound healing process [33]. Thus, biomaterials containing polyphenols can accelerate the wound healing process by the rapid reconstruction of the extracellular matrix. Further, the three polymer networks showed high cell viability for human monocytes observing values higher than 81 ± 9 % after 48 h of incubation. It worth to mention that the polymer networks containing polyphenols showed better performance than IPN-1 which is based on phenol. These results confirm that polyphenols enhance the biocompatibility of this kind of materials. Since the chemical structure of polyphenols is associated with increasing the activity of mitochondrial dehydrogenases in cells, favoring the reduction of MTT salts to formazan.

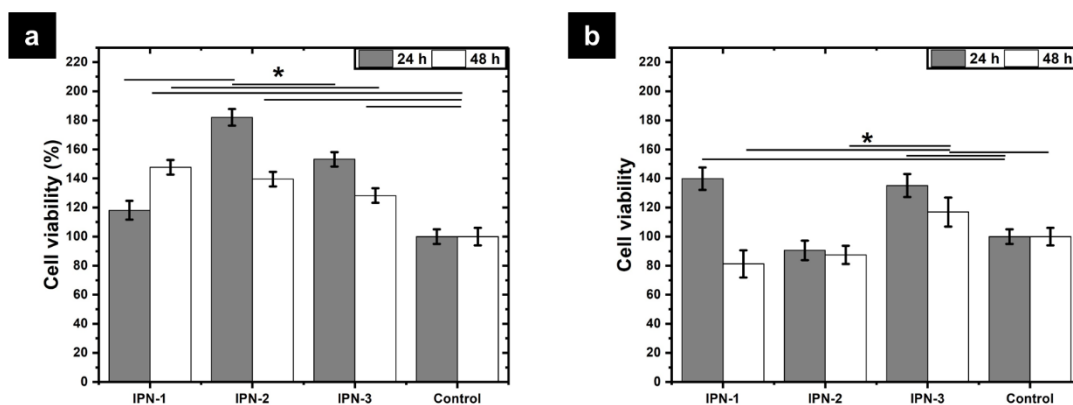


Fig. 8. Cell viability *in vitro* of (a) porcine fibroblasts and (b) human monocytes.

Cell proliferation

Fig. 9 shows images acquired by fluorescence microscopy of human monocytes stained with rhodamine B in contact with polymer networks after incubating for 48 h. The images revealed the presence of large and dense populations of monocytes confirming the biocompatible character of polymer networks observed by the MTT assay.

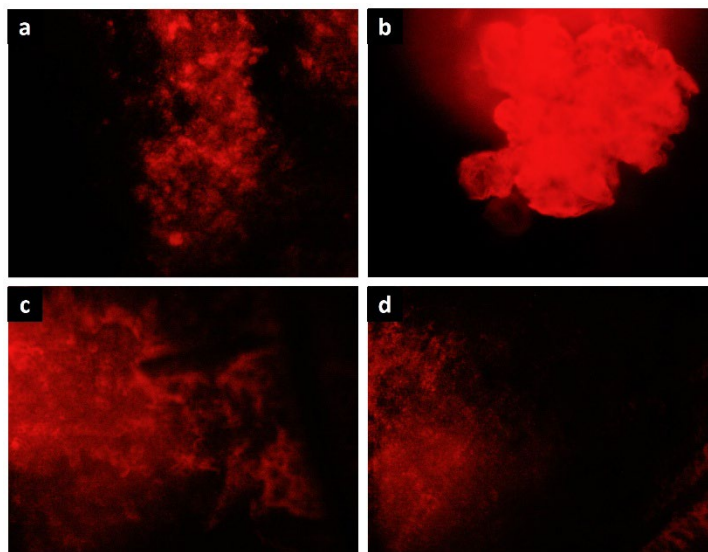


Fig. 9. Human monocytes stained with rhodamine B in contact with polymer networks after 48 h of incubation at 37 °C: (a) PBS-1X, (b) IPN-1, (c) IPN-2, and (d) IPN-3.

Hemolytic activity

The hemolytic activity was measured to evaluate the biocompatibility of phenolic polymer networks in contact with human blood. The hemolytic activity of IPN-1 was 5.9 ± 0.2 % and according to the ASTM-F756 norm is classified as hemolytic. Thus, this IPN is not suitable for being in contact with blood because of it causes damage to cell membrane of erythrocytes. Previously, it was reported that polymer networks comprised only of collagen and polyurethane have not hemolytic character. Thus, the hemolytic character is due to the synthetic phenolic polymer used for interpenetration. Conversely, IPN-2 and IPN-3 has 0 % of hemolytic activity and they are classified as non-hemolytic. Thus, the incorporation of polyphenols from the *Hibiscus sabdariffa* extract in the polymer networks decrease the hemolytic character obtaining new materials with improved hemocompatibility.

According with Cyboran et al., polyphenols have positive effects on erythrocytes increasing their resistance towards changes in the osmotic pressure. This was attributed to the modification of the cell membrane by polyphenols which are retained in the outer lipid monolayer[34]. Further, polyphenols have a protective effect against oxidation induced by free radicals avoiding the effects of cell damage by lipid peroxidation [35-37]. This way, polyphenols are attractive compounds to promote human health with limited side effects.

Cell signaling

It is well known that the intake of polyphenols contained in natural sources helps to modulate chronic inflammatory diseases, such as type 2 diabetes, rheumatoid arthritis, and inflammatory bowel disease, [38]. Also, it was reported that dietary tea polyphenols consumed by rats decreased the serum levels of pro-inflammatory factors such as TNF- α , IL-1 β , and IL-6 showing that polyphenols protected rats from the effects of inflammation and tissue damage caused by fatigue [39]. Polyphenols reduce inflammation by suppressing the pro-inflammatory cytokines such as tumor necrosis factor-alpha (TNF- α) and inducing the apoptosis and decreasing DNA damage. Polyphenols have a potential role in prevention/treatment of inflammatory chronic diseases by regulating signaling pathways and suppressing inflammation. Also, polyphenols cause immunomodulatory effects against allergic reaction and autoimmune disease by inhibition of autoimmune T cell proliferation, and downregulation of pro-inflammatory cytokines [40].

The cell signaling induced by the polymer networks was studied measuring two important cytokines involved in the wound healing process: TNF- α and IL-10, which are related with the inflammatory and anti-inflammatory response, respectively. The inflammatory phase in wound healing is considered as the preparatory process for the formation of new tissue. In this sense, TNF- α may have a beneficial role in wound healing, but

it may have negative effects when it is overexpressed. An excess of TNF- α can inhibited the production of 3-hydroxyproline and thus the production of collagen [41]. Fig. 10(a) shows the concentration of TNF- α secreted by human monocytes after being incubated in contact with polymer networks for 48 h at 37 °C. The concentration of TNF- α was around 50 pg cm⁻³ and significant differences were not observed compared with the control (PBS-1X). The concentration of TNF- α typically founded in human blood is around 10 pg cm⁻³. Thus, IPN-1 and IPN-2 stimulate the secretion of this cytokine without an overexpression showing the beneficial effects of polyphenols for the wound healing process in modulating the inflammatory response. Decreased secretion of TNF- α by monocytes is observed with increasing polyphenol content (IPN-3).

Fig. 10(b) shows the concentration of IL-10 secreted by human monocytes showing a strong stimulation caused by IPN-2. The concentration in the medium was 18600 \pm 700 pg cm⁻³ supering the concentration founded in the control (8150 \pm 215 pg cm⁻³). The overexpression of IL-10 decreases the inflammatory response to injury, creating an environment conducive for regenerative adult wound healing, avoiding the abnormal collagen deposition and promoting the restoration of normal dermal architecture [42]. From the above, polymer networks produced a favorable cell signaling for wound healing, benefiting the proinflammatory response and tissue regeneration. This improvement is suppressed by increasing the content of polyphenols.

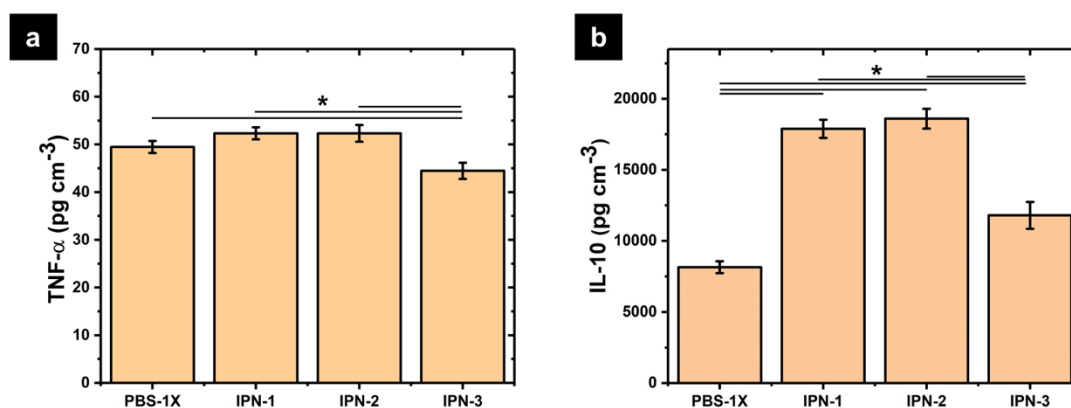


Fig. 10. Secreted cytokines for human monocytes in contact with polymer networks: (a) TNF- α and (b) IL-10.

Conclusions

This study successfully synthesized bio-based polymer networks incorporating polyphenols extracted from *Hibiscus sabdariffa* into phenol-formaldehyde resins. The integration of *Hibiscus sabdariffa* polyphenols partially replaced phenol in the polymer networks, leading to the formation of bio-based interpenetrating polymer networks (IPNs). FTIR analysis confirmed the presence of polyphenols, collagen, and polyurethane in the IPNs. The incorporation of polyphenols resulted in specific bands attributed to glycosylated polyphenols and reduced intensity of phenol-related bands, indicating successful partial substitution. The thermal stability of the IPNs was slightly compromised with the introduction of polyphenols, as evidenced by a decrease in degradation temperatures and residual weight. This was attributed to the lower crosslinking degree and higher oxidation tendency of polyphenols compared to phenol. The IPNs exhibited good biocompatibility, as shown by the MTT assay, hemolysis test, and cell proliferation studies. The materials supported cell viability and demonstrated potential for use in biomedical applications. The polymer networks showed controlled degradation in hydrolytic and proteolytic media, with degradation rates influenced by the pH and enzyme type. This property is crucial for applications requiring biodegradable materials. Overall, the study demonstrates the potential of *Hibiscus sabdariffa* polyphenols as sustainable substitutes for phenol in phenol-formaldehyde resins, offering a pathway to develop environmentally friendly and biocompatible polymer networks with tailored properties for specific applications.

Acknowledgments

The authors thank to Consejo Nacional de Humanidades Ciencia y Tecnología (CONAHCyT) for the financial support (grant FORDECYT-PRONACES/6660/2020).

References

1. Hirano, K.; Asami, M. *React. Funct. Polym.* **2013**, 73, 256–269. DOI: <https://doi.org/10.1016/j.reactfunctpolym.2012.07.003>.
2. Basafa, M.; Hawboldt, K. *Biomass Convers. Biorefinery.* **2021**. DOI: <https://doi.org/10.1007/s13399-021-01408-x>.
3. Briou, B.; Caillol, S.; Robin, J. J.; Lapinte, V. *Eur. J. Lipid Sci. Technol.* **2018**, 120, 1800175.
4. Khezri, R.; Alias, A. B.; Abdul Karim, W. A. W.; Motlagh, S. R. *J. Phys. Conf. Ser.* **2019**, 1349, 012134. DOI: <https://doi.org/10.1088/1742-6596/1349/1/012134>.
5. Sarika, P. R.; Nancarrow, P.; Khansaheb, A.; Ibrahim, T. *Polymers (Basel)*. **2020**, 586, 119543. DOI: <https://doi.org/10.3390/polym12102237>.
6. Biziks, V.; Fleckenstein, M.; Mai, C.; Militz, H. *Holzforchung.* **2020**, 74, 344–350. DOI: <https://doi.org/10.1515/hf-2019-0061>.
7. Hou, J.; Chen, X.; Sun, J.; Fang, Q. *Polymer (Guildf)*. **2020**, 200, 122570. DOI: <https://doi.org/10.1016/j.polymer.2020.122570>.
8. Yang, W.; Rallini, M.; Natali, M.; Kenny, J.; Ma, P.; Dong, W.; Torre, L.; Puglia, D. *Mater. Des.* **2019**, 161, 55–63. DOI: <https://doi.org/10.1016/j.matdes.2018.11.032>.
9. Liu, J.; Dai, J.; Wang, S.; Peng, Y.; Cao, L.; Liu, X. *Compos. Part B Eng.* **2020**, 190, 107926. DOI: <https://doi.org/10.1016/j.compositesb.2020.107926>.
10. Fang, L.; Tao, Y.; Zhou, J.; Wang, C.; Dai, M.; Sun, J.; Fang, Q. *Polym. Chem.* **2021**, 12, 766–770. DOI: <https://doi.org/10.1039/d0py01653e>.
11. De Hoyos-Martínez, P. L.; Issaoui, H.; Herrera, R.; Labidi, J.; Charrier-El Bouhtoury, F. *ACS Sustain. Chem. Eng.* **2021**, 9, 1729–1740. DOI: <https://doi.org/10.1021/acssuschemeng.0c07505>.
12. Hafiz, N. L. M.; Tahir, P. M. D.; Hua, L. S.; Abidin, Z. Z.; Sabaruddin, F. A.; Yunus, N. M.; Abdullah, U. H.; Abdul Khalil, H. P. S. *J. Mater. Res. Technol.* **2020**, 9, 6994–7001. DOI: <https://doi.org/10.1016/j.jmrt.2020.05.029>.
13. Abbas, M.; Saeed, F.; Anjum, F. M.; Afzaal, M.; Tufail, T.; Bashir, M. S.; Ishtiaq, A.; Hussain, S.; Suleria, H. A. R. *Int. J. Food Prop.* **2017**, 20, 1689–1699. DOI: <https://doi.org/10.1080/10942912.2016.1220393>.
14. Aslam, M. S.; Ahmad, M. S.; Riaz, H.; Raza, S. A.; Hussain, S.; Qureshi, O. S.; Maria, P.; Hamzah, Z.; Javed, O. *Phytochemicals.* **2018**, 95–102. DOI: <https://doi.org/http://dx.doi.org/10.5772/intechopen.79179>.
15. Carvalho, M. T. B.; Araújo-Filho, H. G.; Barreto, A. S.; Quintans-Júnior, L. J.; Quintans, J. S. S.; Barreto, R. S. S. *Phytomedicine.* **2021**, 90, 153636. DOI: <https://doi.org/10.1016/j.phymed.2021.153636>.
16. Contardi, M.; Lenzuni, M.; Fiorentini, F.; Summa, M.; Bertorelli, R.; Suarato, G.; Athanassiou, A. *Pharmaceutics* **2021**, 13, 999. DOI: <https://doi.org/10.3390/pharmaceutics13070999>.
17. Tsakiroglou, P.; Vandenakker, N. E.; Del Bo', C.; Riso, P.; Klimis-Zacas, D. *Nutrients.* **2019**, 11, 1075. DOI: <https://doi.org/10.3390/nu11051075>.
18. Riaz, G.; Chopra, R. *Biomed. Pharmacother.* **2018**, 102, 575–586. DOI: <https://doi.org/10.1016/j.biopha.2018.03.023>.
19. Jabeur, I.; Pereira, E.; Caleja, C.; Calhelha, R. C.; Soković, M.; Catarino, L.; Barros, L.; Ferreira, I. C. F. R. *Food Funct.* **2019**, 10, 2234–2243. DOI: <https://doi.org/10.1039/c9fo00287a>.

20. Chou, C. C.; Wang, C. P.; Chen, J. H.; Lin, H. H. *Antioxidants*. **2019**, *8*, 620. DOI: <https://doi.org/10.3390/antiox8120620>.
21. Ali, B. H.; Al Wabel, N.; Blunden, G. *Phyther. Res.* **2005**, *19*, 369–375. DOI: <https://doi.org/10.1002/ptr.1628>.
22. Cavalcante, J.; Oldal, D. G.; Peskov, M. V.; Beke, A. K.; Hardian, R.; Schwingenschlögl, U.; Szekeley, G. *ACS Nano* **2024**, *18*, 7433–7443. DOI: <https://doi.org/10.1021/acsnano.3c10827>.
23. Dutta, S.; Gupta, R. Sen; Manna, K.; Islam, S. S.; Bose, S. *Chem. Eng. J.* **2023**, *472*, 145008. DOI: <https://doi.org/10.1016/j.cej.2023.145008>.
24. Zhao, D.; Kim, J. F.; Ignacz, G.; Pogany, P.; Lee, Y. M.; Szekeley, G. *ACS Nano*. **2019**, *13*, 125–133. DOI: <https://doi.org/10.1021/acsnano.8b04123>.
25. Wancura, M.; Nkansah, A.; Chwatko, M.; Robinson, A.; Fairley, A.; Cosgriff-Hernandez, E. *J. Mater. Chem. B*. **2023**, *11*, 5416–5428. DOI: <https://doi.org/10.1039/d2tb02825e>.
26. Claudio-Rizo, J. A.; Carrillo-Cortés, S. L.; Becerra-Rodríguez, J. J.; Caldera-Villalobos, M.; Cabrera-Munguía, D. A.; Burciaga-Montemayor, N. G. *J. Mater. Res.* **2022**, *37*, 636–649. DOI: <https://doi.org/10.1557/s43578-021-00476-z>.
27. Claudio-Rizo, J. A.; Escobedo-Estrada, N.; Carrillo-Cortés, S. L.; Cabrera-Munguía, D. A.; Flores-Guía, T. E.; Becerra-Rodríguez, J. J. *J. Mater. Sci. Mater. Med.* **2021**, *32*. DOI: <https://doi.org/10.1007/s10856-021-06544-4>.
28. Zhang, W.; Qi, X.; Zhao, Y.; Liu, Y.; Xu, L.; Song, X.; Xiao, C.; Yuan, X.; Zhang, J.; Hou, M. *Int. J. Pharm.* **2020**, *586*, 119543. DOI: <https://doi.org/10.1016/j.ijpharm.2020.119543>.
29. Ragupathi Raja Kannan, R.; Arumugam, R.; Anantharaman, P. *Curr. Bioact. Compd.* **2011**, *7*, 118–125. DOI: <https://doi.org/10.2174/157340711796011142>.
30. Lee, M. Y.; Yoo, M. S.; Whang, Y. J.; Jin, Y. J.; Hong, M. H.; Pyo, Y. H. *Korean J. Food Sci. Technol.* **2012**, *44*, 540–544. DOI: <https://doi.org/10.9721/KJFST.2012.44.5.540>.
31. Márquez-Rodríguez, A. S.; Grajeda-Iglesias, C.; Sánchez-Bojorge, N. A.; Figueroa-Espinoza, M. C.; Rodríguez-Valdez, L. M.; Fuentes-Montero, M. E.; Salas, E. *Molecules*. **2018**, *23*, 1587. DOI: <https://doi.org/10.3390/molecules23071587>.
32. Guimarães, I.; Baptista-Silva, S.; Pintado, M.; Oliveira, A. L. *Appl. Sci.* **2021**, *11*, 1230. DOI: <https://doi.org/10.3390/app11031230>.
33. Chowdhury, A.; Nosoudi, N.; Karamched, S.; Parasaram, V.; Vyavahare, N. *Polyphenol J. Dermatol. Sci.* **2021**, *102*, 94–100. DOI: <https://doi.org/10.1016/j.jdermsci.2021.03.002>.
34. Cyboran, S.; Oszmiański, J.; Kleszczyńska, H. *Cell. Mol. Biol. Lett.* **2012**, *17*, 77–88. DOI: <https://doi.org/10.2478/s11658-011-0038-4>.
35. Krishna, P. G. A.; Sivakumar, T. R.; Jin, C.; Li, S. H.; Weng, Y. J.; Yin, J.; Jia, J.-Q.; Wang, C. Y.; Gui, Z. Z. *Pharmacogn. Mag.* **2018**, *14*, 103. DOI: <https://doi.org/10.4103/pm.pm>.
36. Kaviarasan, S.; Vijayalakshmi, K.; Anuradha, C. V. *Plant Foods Hum. Nutr.* **2004**, *59*, 143–147. DOI: <https://doi.org/10.1007/s11130-004-0025-2>.
37. Lanping, M. A.; Zaiqun, L. I. U.; Bo, Z.; Li, Y.; Zhongli, L. I. U. *Chinese Sci. Bull.* **2000**, *45*, 2052–2056.
38. Kawaguchi, K.; Matsumoto, T.; Kumazawa, Y. *Curr. Top. Med. Chem.* **2011**, *11*, 1767–1779. DOI: <https://doi.org/10.2174/156802611796235152>.
39. Liu, L.; Wu, X.; Zhang, B.; Yang, W.; Li, D.; Dong, Y.; Yin, Y.; Chen, Q. *Food Nutr. Res.* **2017**, *61*, 1333390. DOI: <https://doi.org/10.1080/16546628.2017.1333390>.
40. Shakoob, H.; Feehan, J.; Apostolopoulos, V.; Platat, C.; Dhaheri, A. S. Al; Ali, H. I.; Ismail, L. C.; Bosevski, M.; Stojanovska, L. *Nutrients* **2021**, *13*, 728. DOI: <https://doi.org/10.3390/nu13030728>.
41. Rapala, K. *Ann. Chir. Gynaecol. Suppl.* **1996**, *211*, 1–53.
42. Peranteau, W. H.; Zhang, L.; Muvarak, N.; Badillo, A. T.; Radu, A.; Zoltick, P. W.; Liechty, K. W. *J. Invest. Dermatol.* **2008**, *128*, 1852–1860. DOI: <https://doi.org/10.1038/sj.jid.5701232>.